

# Chapter 10

Gibbs Free Energy Composition and Phase  
Diagrams of Binary Systems

## 10.2 Gibbs Free Energy and Thermodynamic Activity

The Gibbs free energy of mixing of the components A and B to form a mole of solution:

$$\Delta G^M = RT(X_A \ln a_A + X_B \ln a_B)$$

If it is ideal, i.e., if  $a_i = X_i$ , then the molar Gibbs free energy of mixing,

$$\Delta G^{M,id} = RT(X_A \ln X_A + X_B \ln X_B)$$

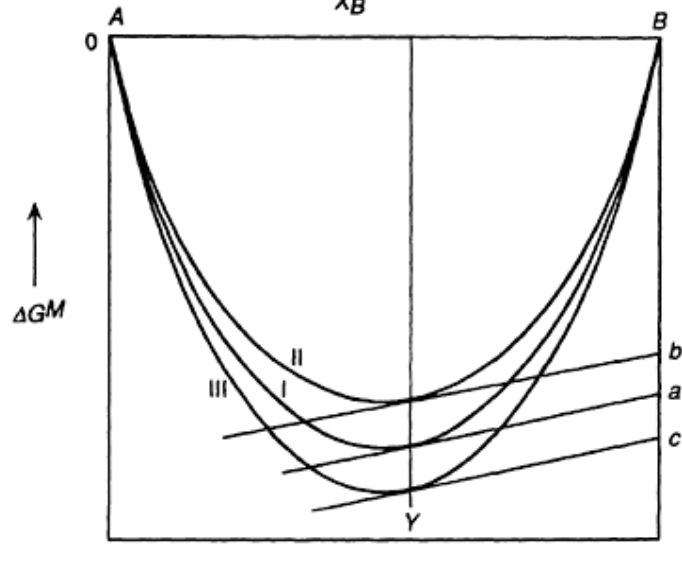


**Figure 10.1** The molar Gibbs free energies of mixing in binary systems exhibiting ideal behavior (I), positive deviation from ideal behavior (II), and negative deviation from ideal behavior (III).

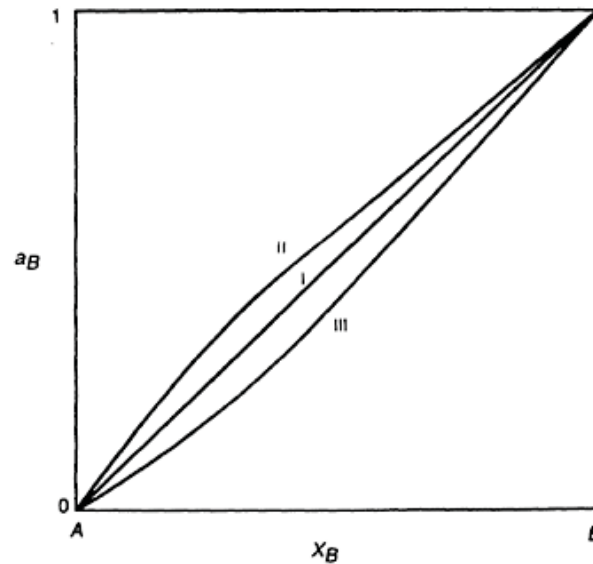


**Figure 10.2** The activities of component B obtained from lines I, II, and III in Fig. 10.1.

$$|Bb = \Delta \bar{G}_B^M = RT \ln a_B \text{ (in system II)}| < |Ba = \Delta \bar{G}_B^M = RT \ln X_B| \\ < |Bc = \Delta \bar{G}_B^M = RT \ln a_B \text{ (in system III)}|$$

$$\gamma_B \text{ in system II} > 1 > \gamma_B \text{ in system III}$$

## 10.3 The Gibbs Free Energy of Formation of Regular Solutions

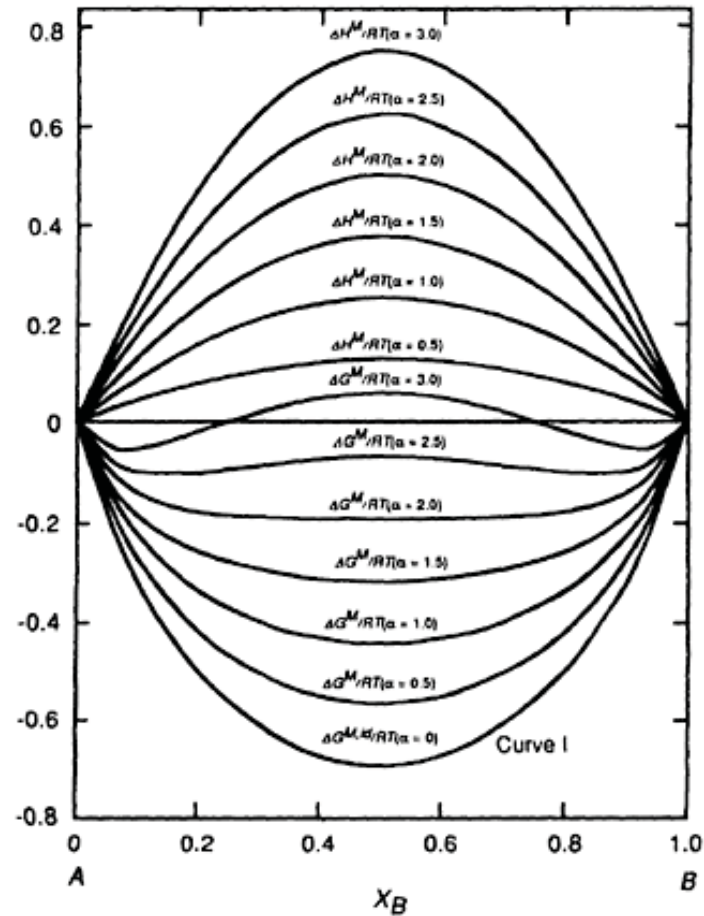


**Figure 10.3** The effect of the magnitude of  $\alpha$  on the integral molar heats and integral molar Gibbs free energies of formation of a binary regular solution.

If curves II and III for regular solutions, then deviation of  $\Delta G^M$  from  $\Delta G^{M,id}$  is

$$= G^{XS} = RT\alpha X_A X_B = \Omega X_A X_B = \Delta H^M$$

For curve II,  $|\Delta G^M| < |\Delta G^{M,id}|$ , and thus  $\Delta H^M$  is a positive quantity ( $\alpha$  and  $\Omega$  are positive quantities).

## 10.3 The Gibbs Free Energy of Formation of Regular Solutions

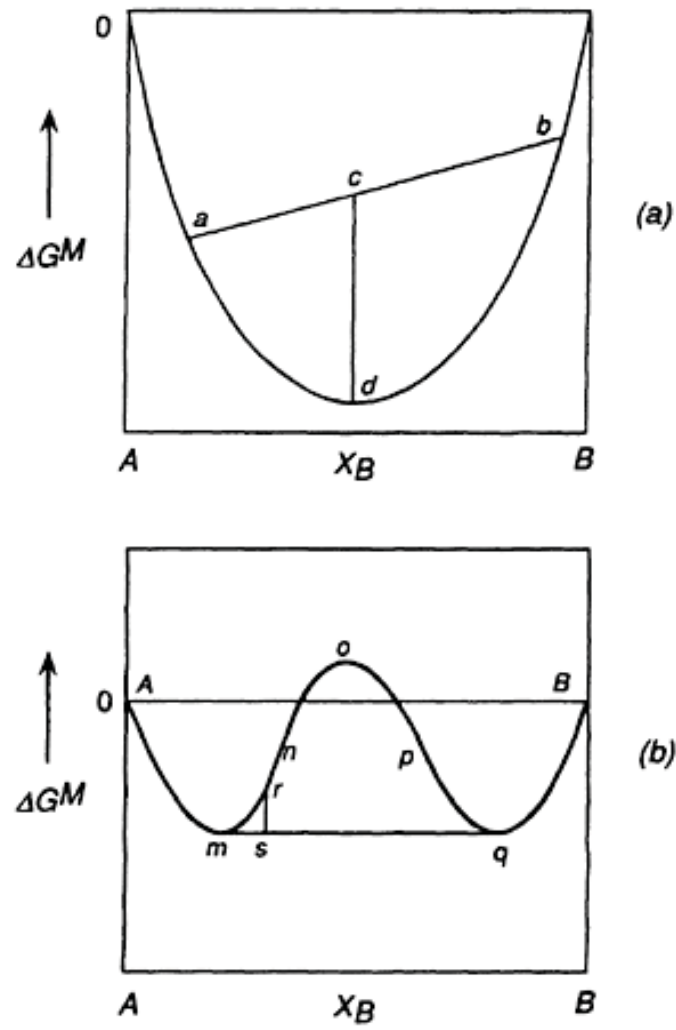


**Figure 10.4** (a) The molar Gibbs free energies of mixing of binary components which form a complete range of solutions. (b) The molar Gibbs free energies of mixing of binary components in a system which exhibits a miscibility gap.

# 10.4 Criteria for Phase Stability in Regular Solutions

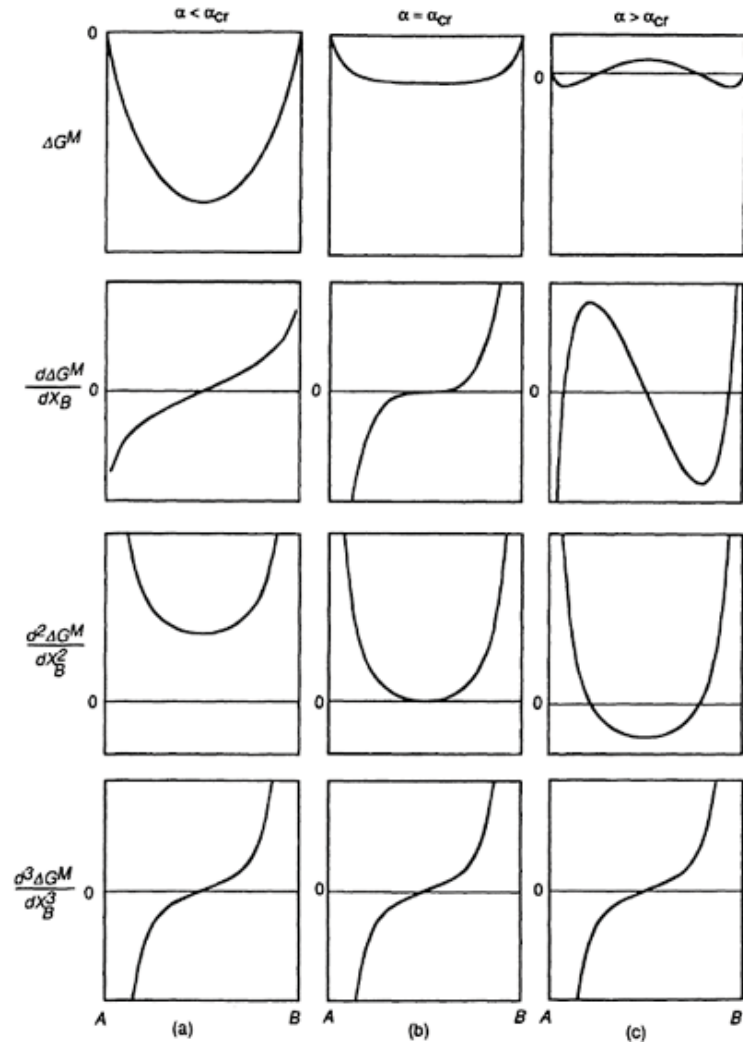
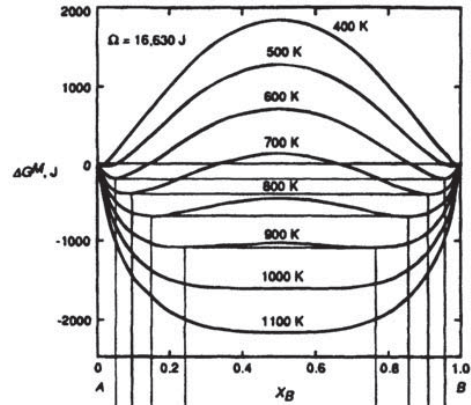


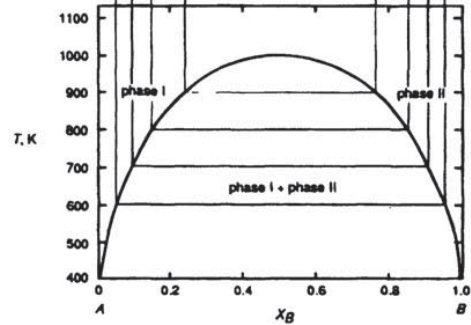
**Figure 10.5** The effect of the magnitude of  $\alpha$  on the first, second, and third derivatives of the integral Gibbs free energy of mixing with respect to composition.



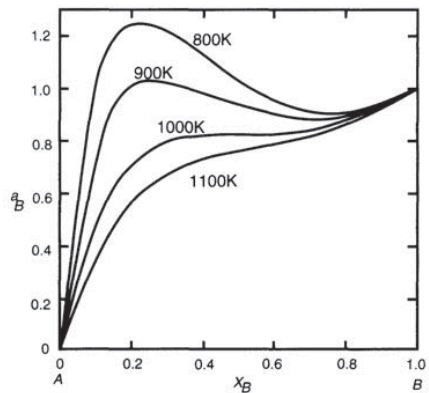
# 10.4 Criteria for Phase Stability in Regular Solutions



(a)



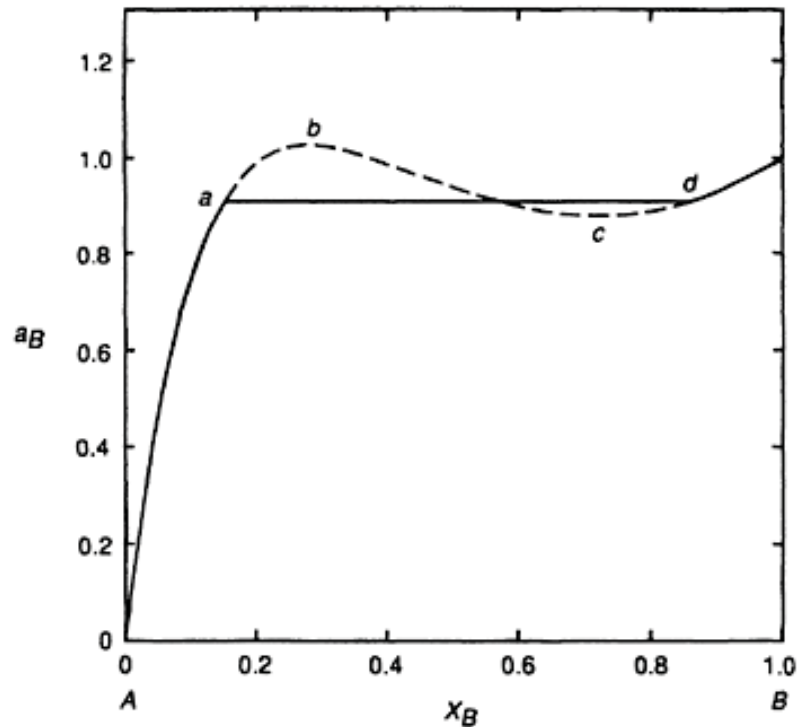
(b)



(c)

**Figure 10.6** (a) The effect of temperature on the molar Gibbs free energy of mixing a binary regular solution for which  $\Omega=16,630$  joules, (b) The loci of the double tangent points in (a), which generate the phase diagram for the system, (c). The activities of component B derived from (a).

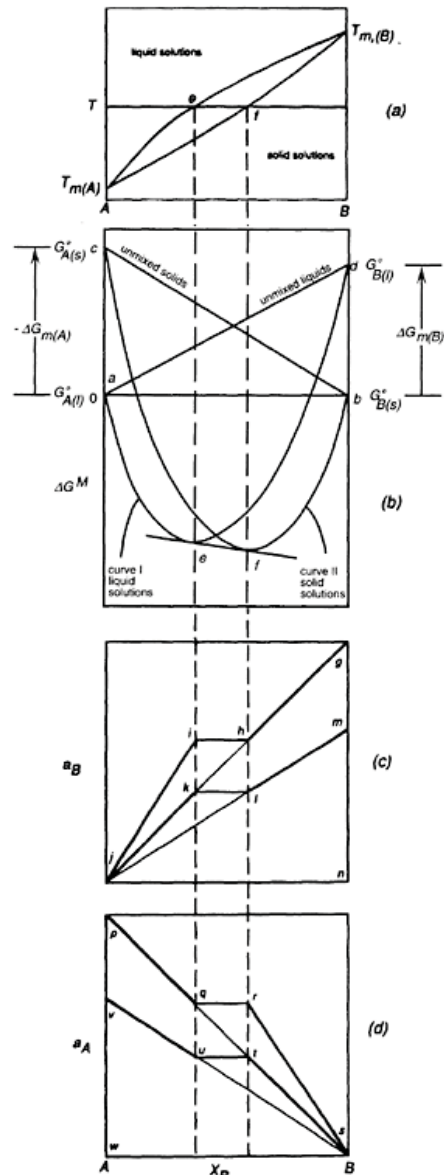
## 10.4 Criteria for Phase Stability in Regular Solutions



The derived activity curve between  $b$  and  $c$ , and, consequently, the Gibbs free energy of mixing curve between the spinodal compositions, have no physical significance. The horizontal line drawn between  $a$  and  $d$  in **Fig. 10.7** represents the actual constant activity of  $B$  in the two-phase region, and the compositions  $a$  and  $d$  are those of the double tangents to the Gibbs free energy of mixing curve.

**Figure 10.7** The activity of  $B$  at 800 K derived from Fig. 10.6a.

# 10.5 Liquid and Solid Standard States



Consider the binary system  $A-B$  at a temperature  $T$  which is below  $T_m(B)$ , the melting temperature of  $B$ , and above  $T_m(A)$ , the melting temperature of  $A$ . Consider, further, that this system forms Raoultian ideal liquid solutions and Raoultian ideal solid solutions. The phase diagram for the system and the temperature of interest,  $T$ , are shown in Fig. 10.8a. Fig. 10.8b shows the two Gibbs free energy of mixing curves of interest, curve I drawn for liquid solutions and curve II drawn for solid solutions. At the temperature  $T$ , the stable states of pure  $A$  and  $B$  are located at  $\Delta G^M=0$ , with pure liquid  $A$  located at  $X_A=1$  (the point  $a$ ) and pure solid  $B$  located at  $X_B=1$  (the point  $b$ ). The point  $c$  represents the molar Gibbs free energy of solid  $A$  relative to that of liquid  $A$  at the temperature  $T$ , and  $T > T_m(A)$ , then  $G_{A(s)}^0 - G_{A(l)}^0$  is a positive quantity which is equal to the negative of the molar Gibbs free energy of melting of  $A$  at the temperature  $T$ . That is,

$$G_{A(s)}^0 - G_{A(l)}^0 = -\Delta G_{m(A)}^0 = -(\Delta H_{m(A)}^0 - T\Delta S_{m(A)}^0)$$

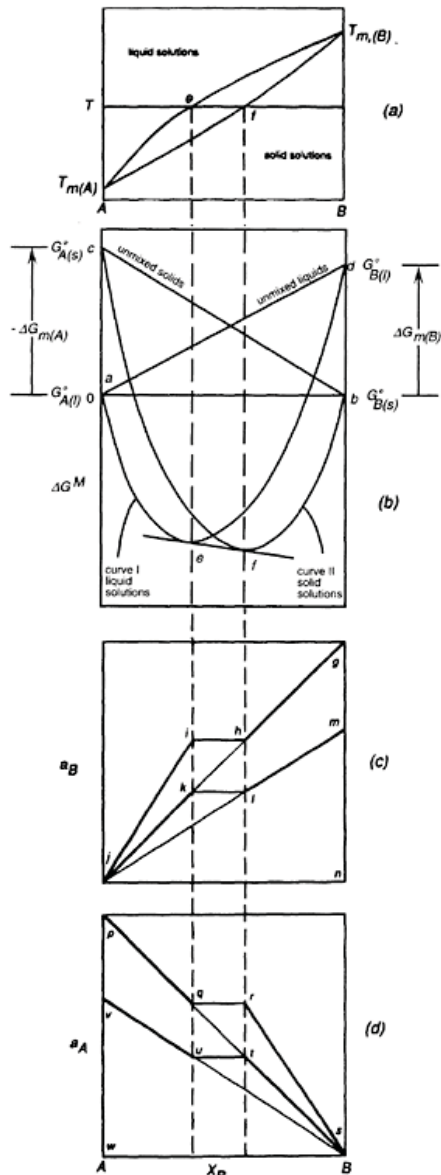
and if  $c_{p,A(s)} = c_{p,A(l)}$  that is, if  $\Delta H_{m(A)}^0$  and  $\Delta S_{m(A)}^0$  are independent of temperature, then

$$\Delta G_{m(A)}^0 = \Delta H_{m(A)}^0 \left( \frac{T_m(A) - T}{T_m(A)} \right) \quad (10.4)$$

**Figure 10.8** (a) The phase diagram for the system  $A-B$ . (b) The Gibbs free energies of mixing in the system  $A-B$  at the temperature  $T$ . (c) The activities of  $B$  at the temperature  $T$  and comparison of the solid and liquid standard states, (d) The activities of  $A$  at the temperature  $T$ , and comparison of the solid and liquid standard states.



# 10.5 Liquid and Solid Standard States



At any composition the formation of a homogeneous liquid solution from pure liquid A and pure solid B can be considered as being a two-step process involving

1. The melting of  $X_B$  moles of B, which involves the change in Gibbs free energy  $\Delta G = X_B \Delta G_{m(B)}^0$ , and
2. The mixing of  $X_B$  moles of liquid B and  $X_A$  moles of liquid A to form an ideal liquid solution, which involves the change in Gibbs free energy,

Thus, the molar Gibbs free energy of formation of an ideal liquid solution,  $\Delta G_{(l)}^M$ , from liquid A and solid B is give by

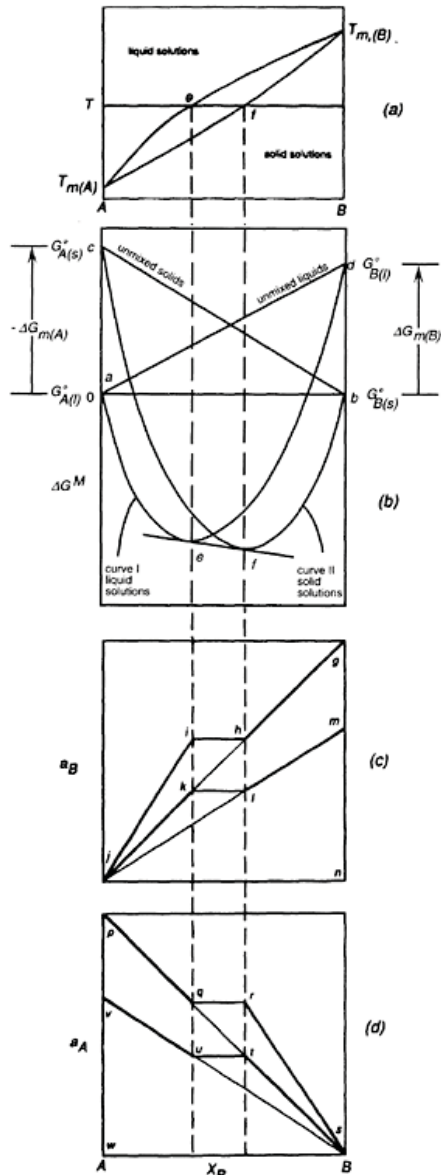
$$\Delta G_{(l)}^M = RT(X_A \ln X_A + X_B \ln X_B) + X_B \Delta G_{m(B)}^0 \quad (10.5)$$

Similarly

$$\Delta G_{(s)}^M = RT(X_A \ln X_A + X_B \ln X_B) - X_A \Delta G_{m(A)}^0 \quad (10.6)$$

**Figure 10.8** (a) The phase diagram for the system A–B. (b) The Gibbs free energies of mixing in the system A–B at the temperature  $T$ . (c) The activities of B at the temperature  $T$  and comparison of the solid and liquid standard states, (d) The activities of A at the temperature  $T$ , and comparison of the solid and liquid standard states.

# 10.5 Liquid and Solid Standard States



For equilibrium between the solid and liquid phases,

$$\Delta \bar{G}_A^M \text{ (in the solid solution)} = \Delta \bar{G}_A^M \text{ (in the liquid solution)} \quad (10.7)$$

and

$$\Delta \bar{G}_B^M \text{ (in the liquid solution)} = \Delta \bar{G}_B^M \text{ (in the solid solution)} \quad (10.8)$$

At any temperature  $T$ , these two conditions fix the solidus and liquidus compositions, i.e., the position of the points of double tangency. From Eq. (10.5)

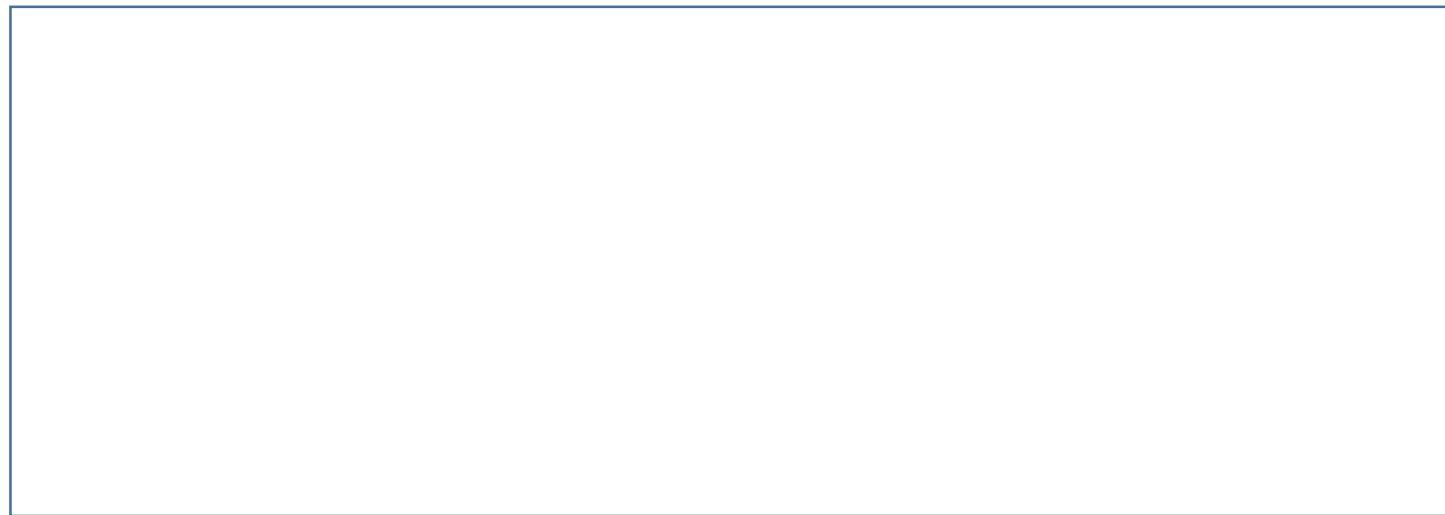


**Figure 10.8** (a) The phase diagram for the system  $A-B$ . (b) The Gibbs free energies of mixing in the system  $A-B$  at the temperature  $T$ . (c) The activities of  $B$  at the temperature  $T$  and comparison of the solid and liquid standard states, (d) The activities of  $A$  at the temperature  $T$ , and comparison of the solid and liquid standard states.

# 10.5 Liquid and Solid Standard States

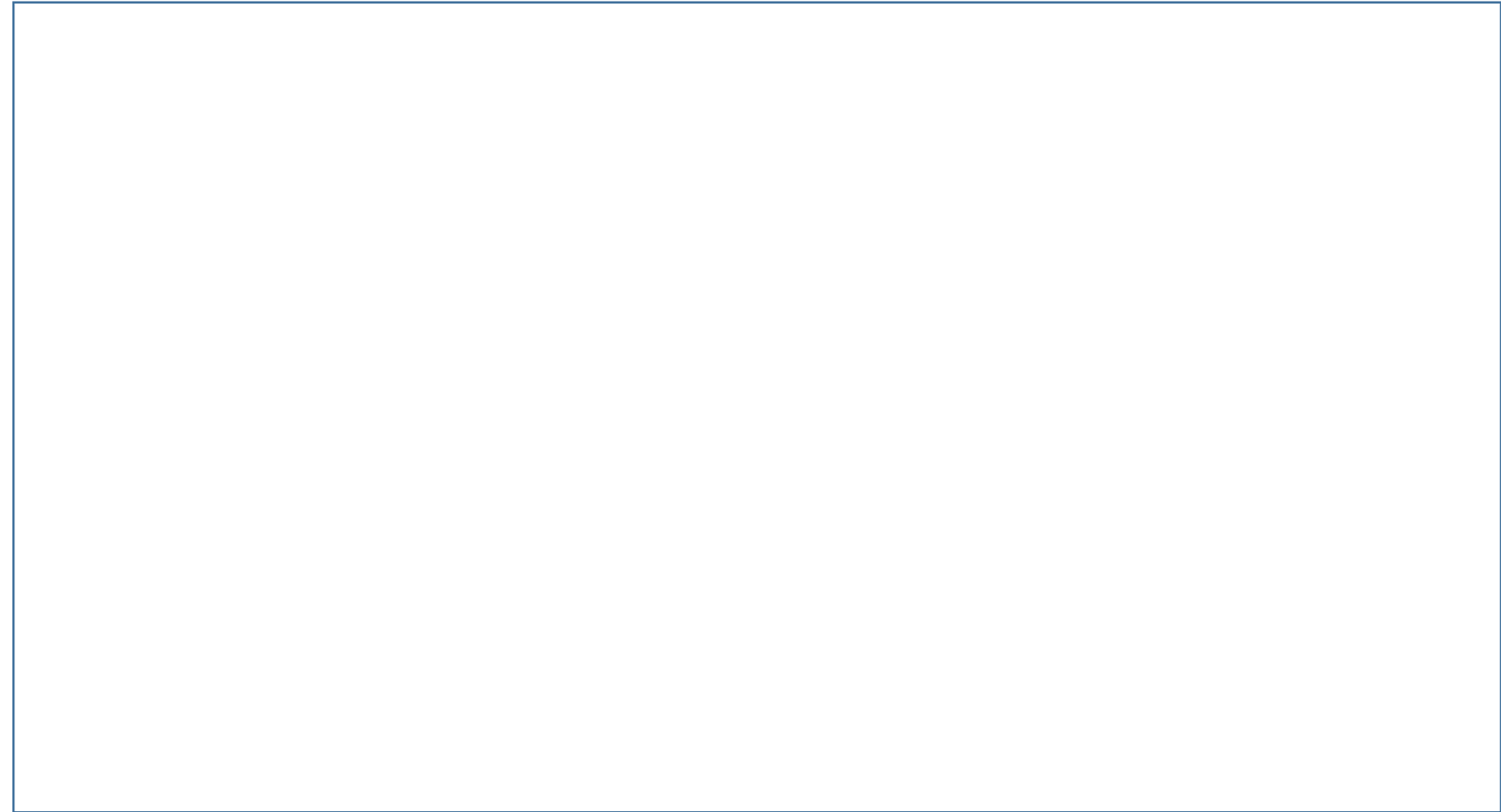
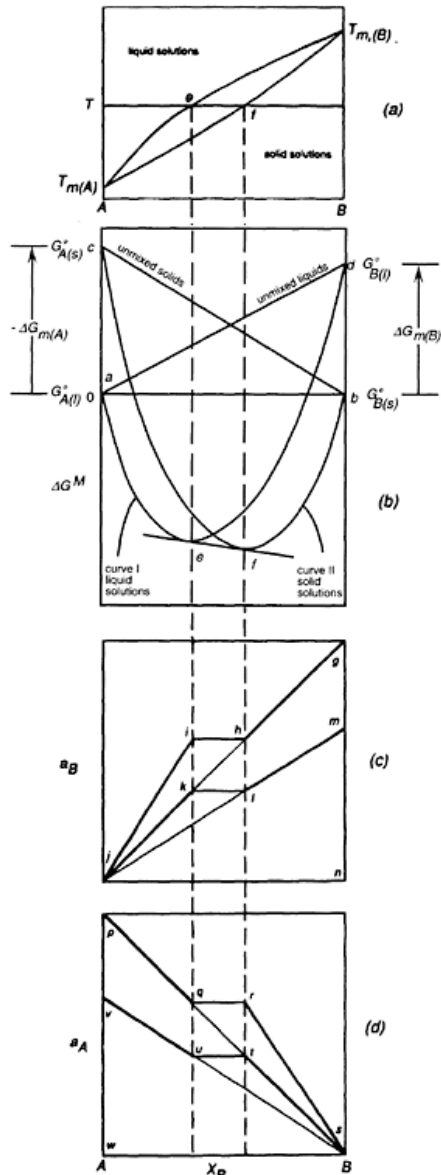


**Figure 10.8** (a) The phase diagram for the system  $A-B$ . (b) The Gibbs free energies of mixing in the system  $A-B$  at the temperature  $T$ . (c) The activities of  $B$  at the temperature  $T$  and comparison of the solid and liquid standard states, (d) The activities of  $A$  at the temperature  $T$ , and comparison of the solid and liquid standard states.

# 10.5 Liquid and Solid Standard States

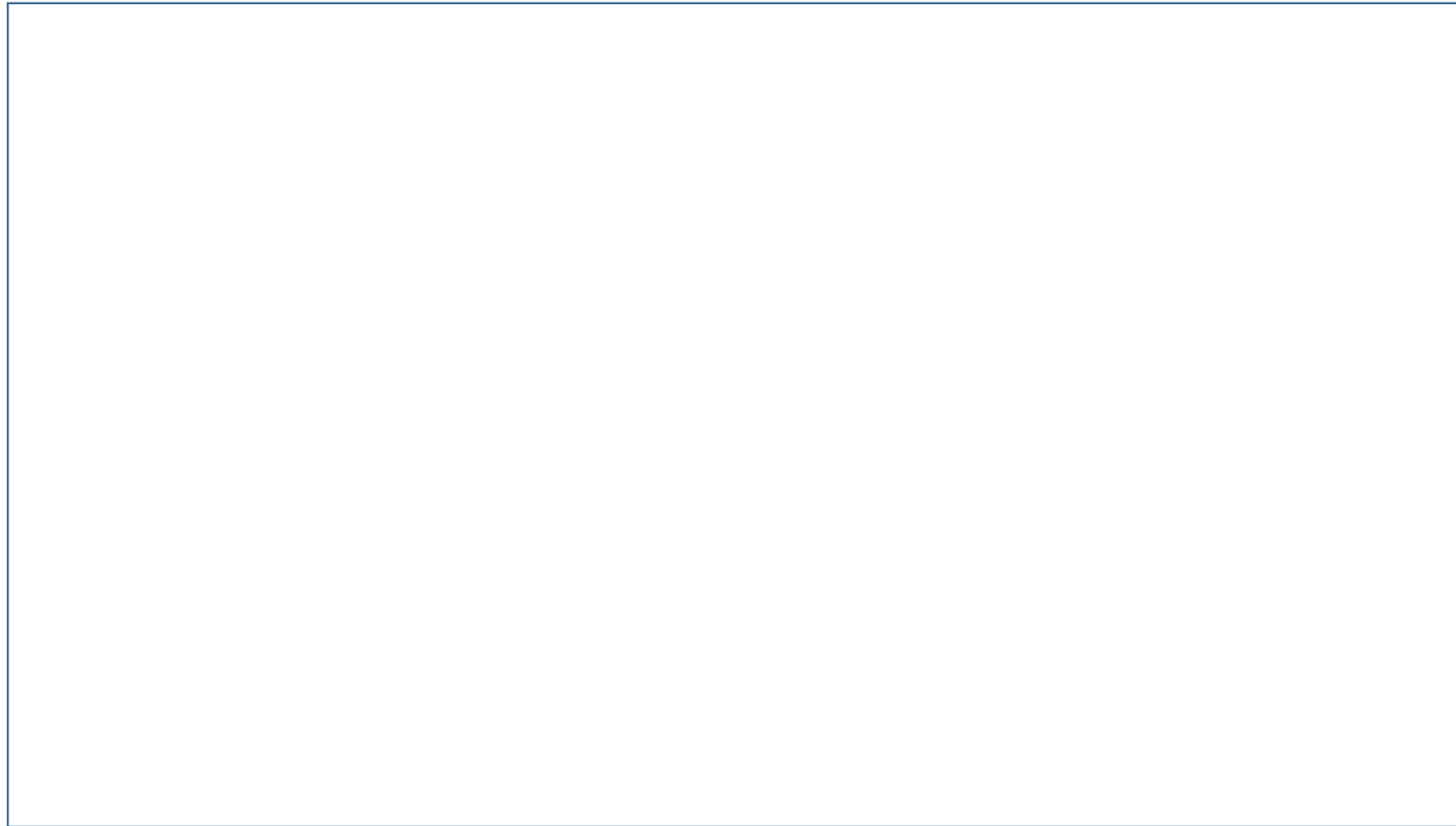
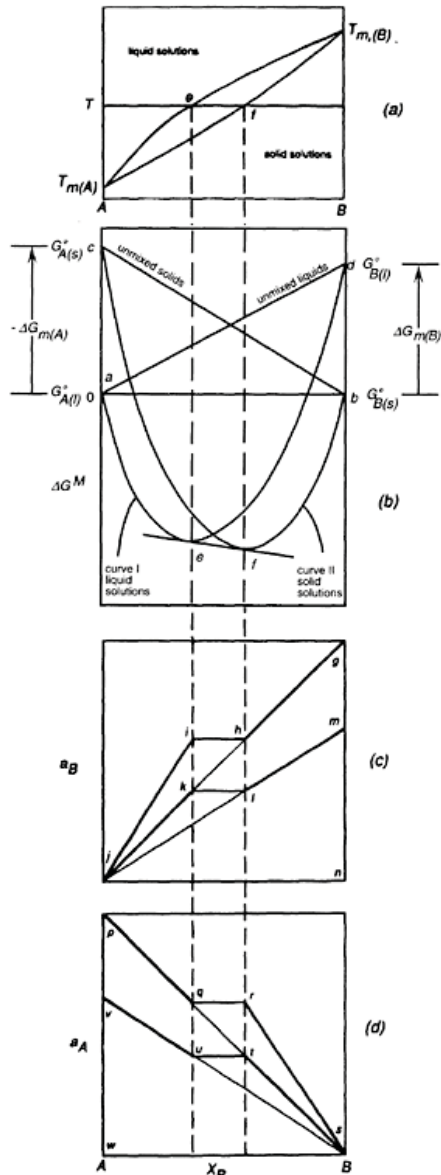


**Figure 10.8** (a) The phase diagram for the system  $A-B$ . (b) The Gibbs free energies of mixing in the system  $A-B$  at the temperature  $T$ . (c) The activities of  $B$  at the temperature  $T$  and comparison of the solid and liquid standard states, (d) The activities of  $A$  at the temperature  $T$ , and comparison of the solid and liquid standard states.

# 10.5 Liquid and Solid Standard States

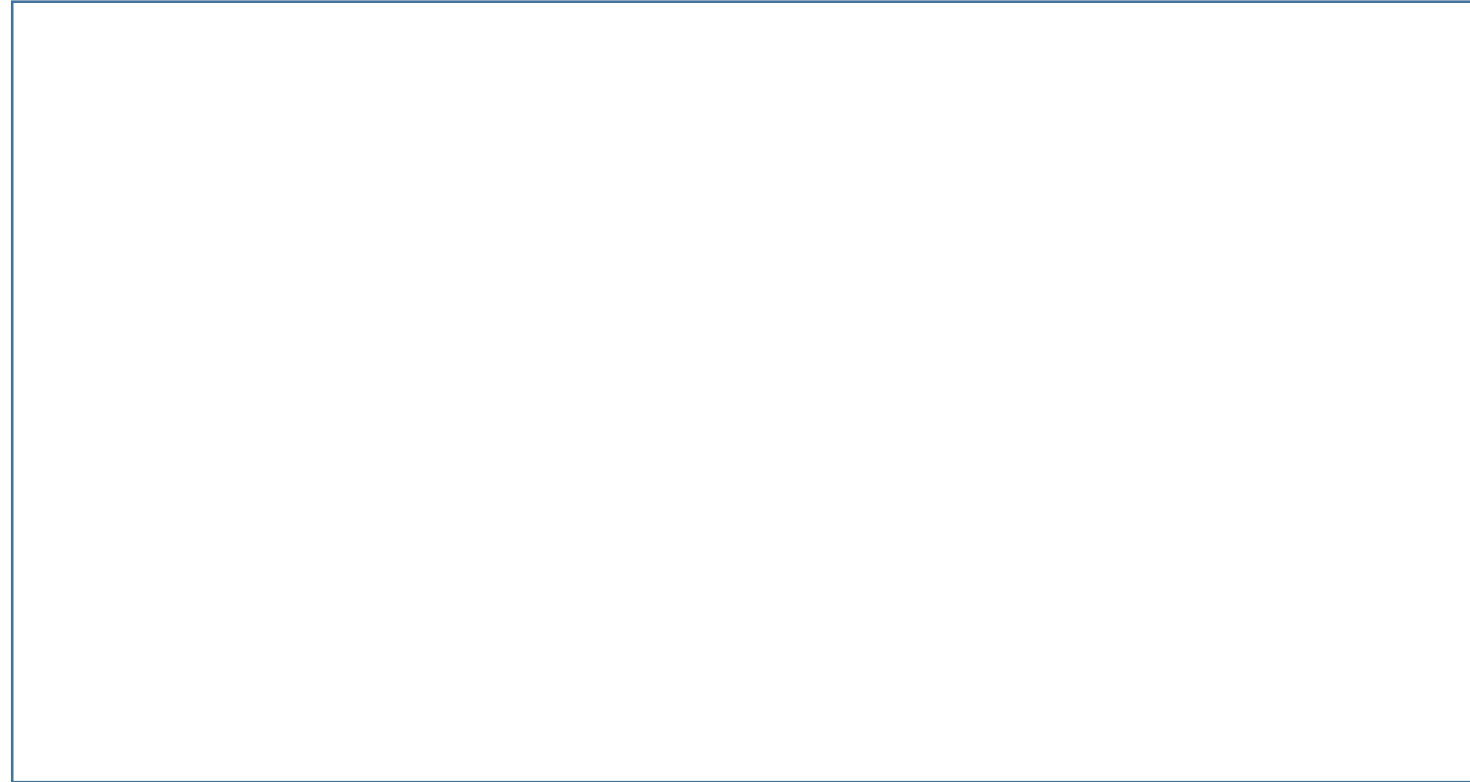
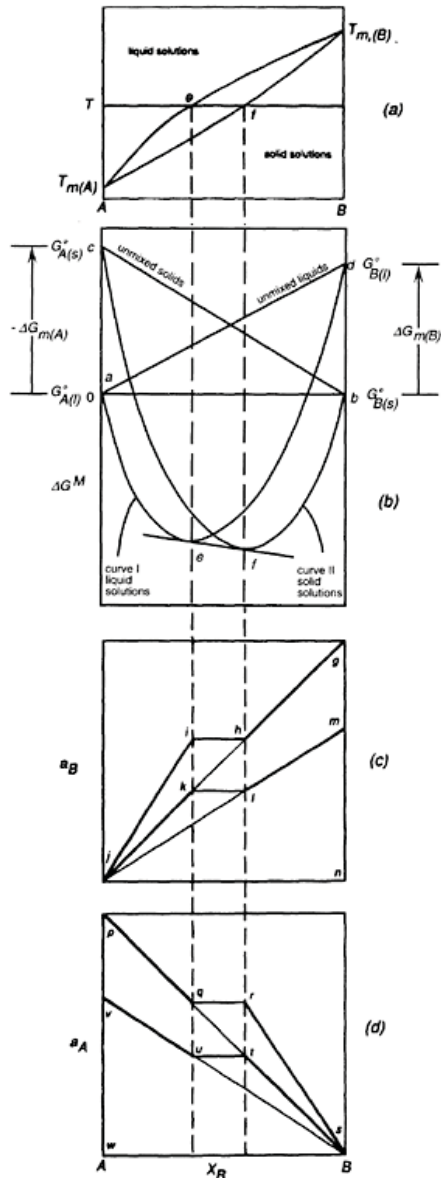
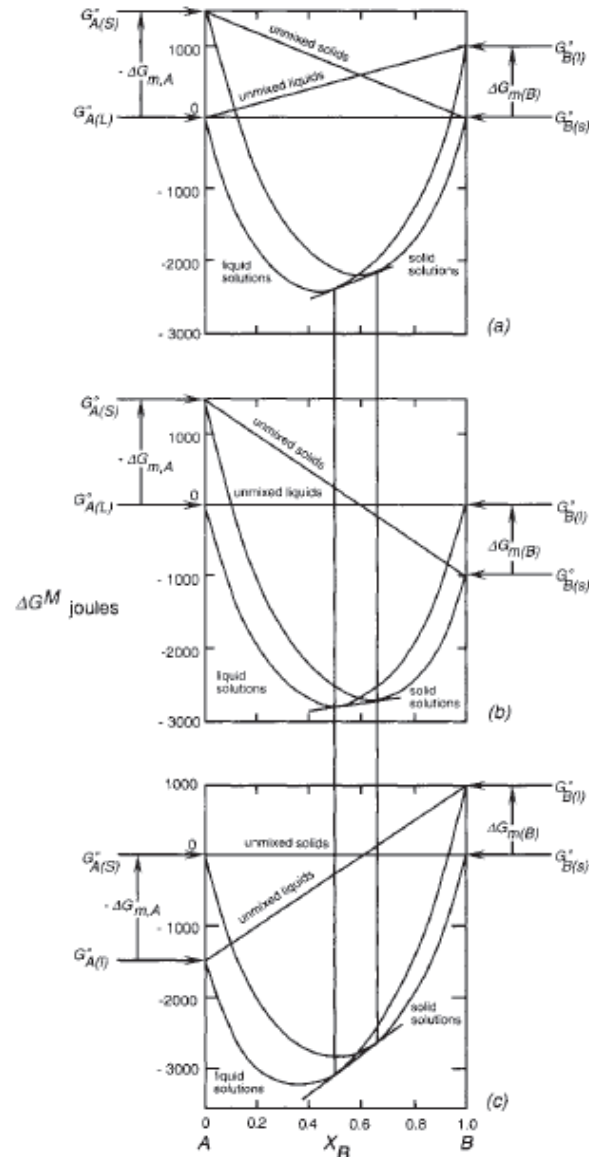


**Figure 10.8** (a) The phase diagram for the system  $A-B$ . (b) The Gibbs free energies of mixing in the system  $A-B$  at the temperature  $T$ . (c) The activities of  $B$  at the temperature  $T$  and comparison of the solid and liquid standard states, (d) The activities of  $A$  at the temperature  $T$ , and comparison of the solid and liquid standard states.

# 10.5 Liquid and Solid Standard States



Comparison among the three shows that, because of the logarithmic nature of the Gibbs free energy curves, the positions of the points of double tangency **are not influenced by the choice of standard state**; they are determined only by the temperature  $T$  and by the magnitude of the difference between  $G_{(l)}^0$  and  $G_{(s)}^0$  for both components at the temperature  $T$ .

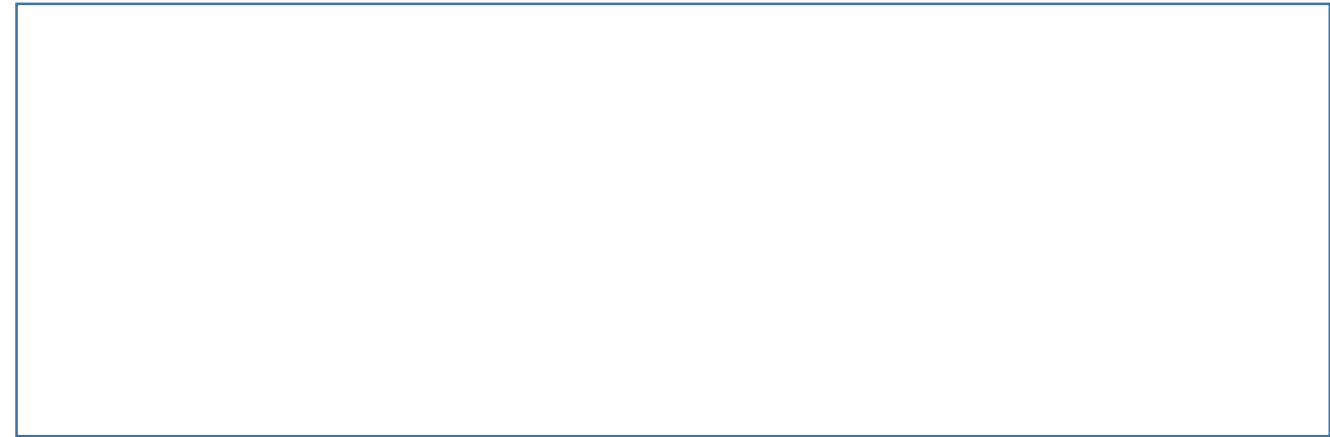
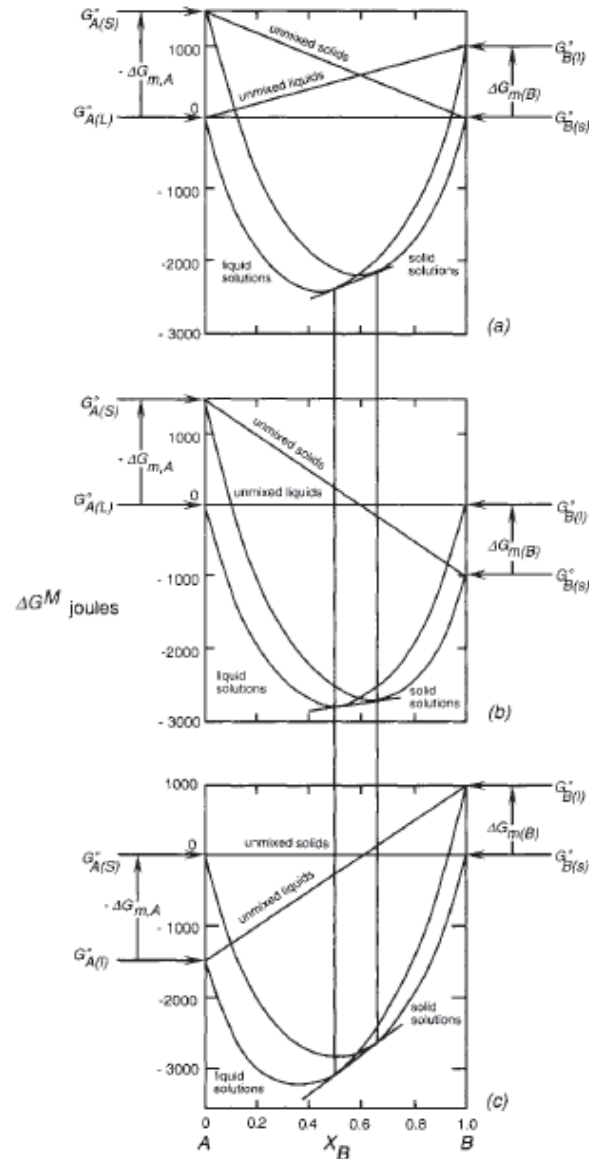


**Figure 10.10** The Gibbs free energy of mixing curves for a binary system  $A$ – $B$  which forms ideal solid solutions and ideal liquid solutions, at a temperature which is higher than  $T_m(A)$  and lower than  $T_m(B)$ . (a) Liquid  $A$  and solid  $B$  chosen as standard states located at  $\Delta G^M=0$ . (b) Liquid  $A$  and liquid  $B$  chosen as standard states located at  $\Delta G^M=0$ . (c) Solid  $A$  and solid  $B$  chosen as standard states located at  $\Delta G^M=0$ . The positions of the points of double tangency are not influenced by the choice of standard state.

# 10.5 Liquid and Solid Standard States



$$\frac{a_i \text{ with respect to solid } i}{a_i \text{ with respect to liquid } i} = \exp\left(\frac{\Delta G_{m(i)}^0}{RT}\right)$$

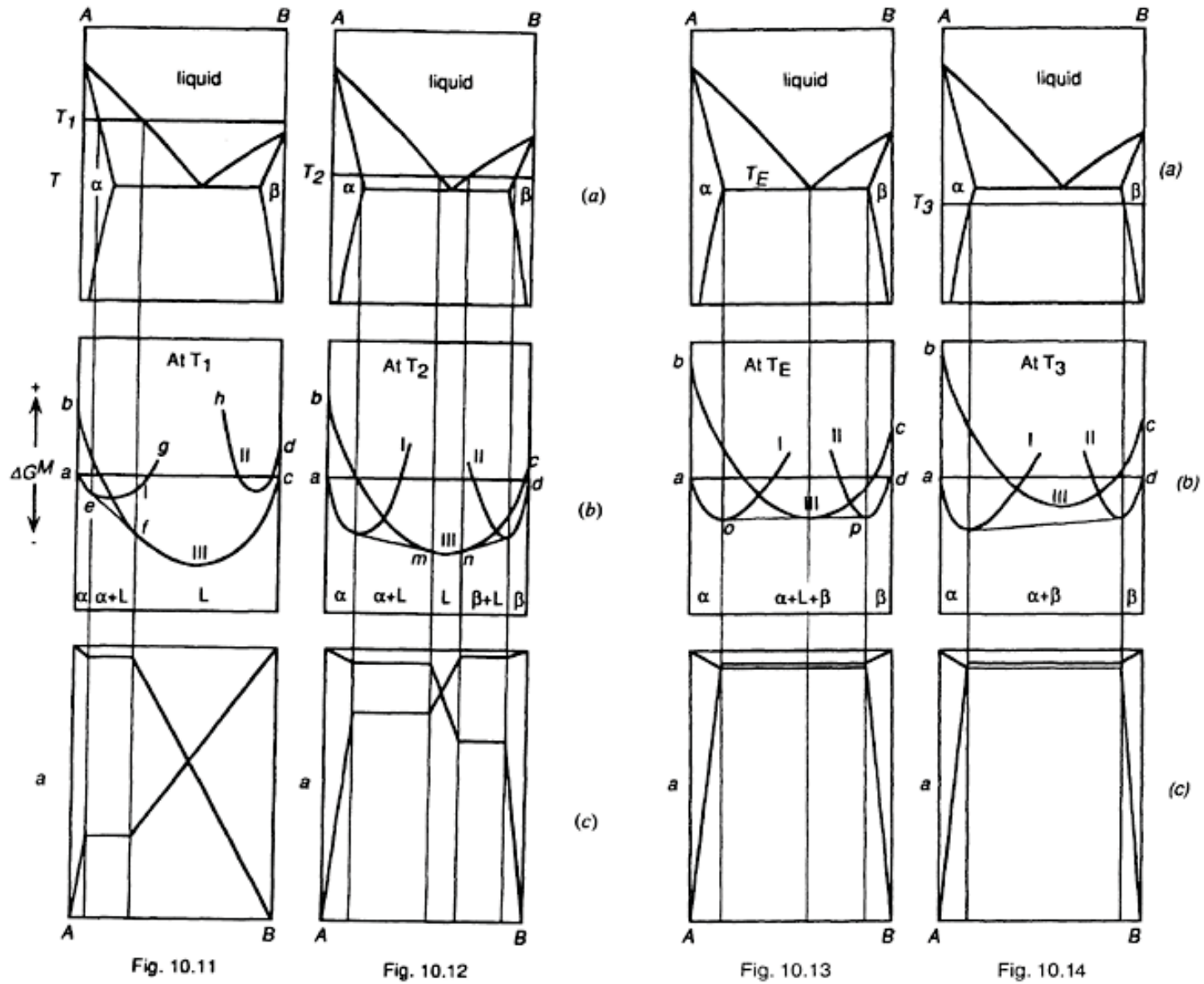
which, from Eq. (10.4),

$$= \exp\left[\Delta H_{m(i)}^0 \left(\frac{T_{m(i)} - T}{RT_{m(i)}}\right)\right] \quad (10.22)$$

In Fig. 10.8, at the temperature  $T_m(B)$ , solid and liquid  $B$  coexist in equilibrium,  $\Delta G_{m(A)}^0 = 0$  and the points  $p$  and  $v$  coincide. Similarly, at the temperature  $T_m(B)^0$  the points  $m$  and  $g$  coincide.

**Figure 10.10** The Gibbs free energy of mixing curves for a binary system  $A$ – $B$  which forms ideal solid solutions and ideal liquid solutions, at a temperature which is higher than  $T_m(A)$  and lower than  $T_m(B)$ . (a) Liquid  $A$  and solid  $B$  chosen as standard states located at  $\Delta G^M = 0$ . (b) Liquid  $A$  and liquid  $B$  chosen as standard states located at  $\Delta G^M = 0$ . (c) Solid  $A$  and solid  $B$  chosen as standard states located at  $\Delta G^M = 0$ . The positions of the points of double tangency are not influenced by the choice of standard state.

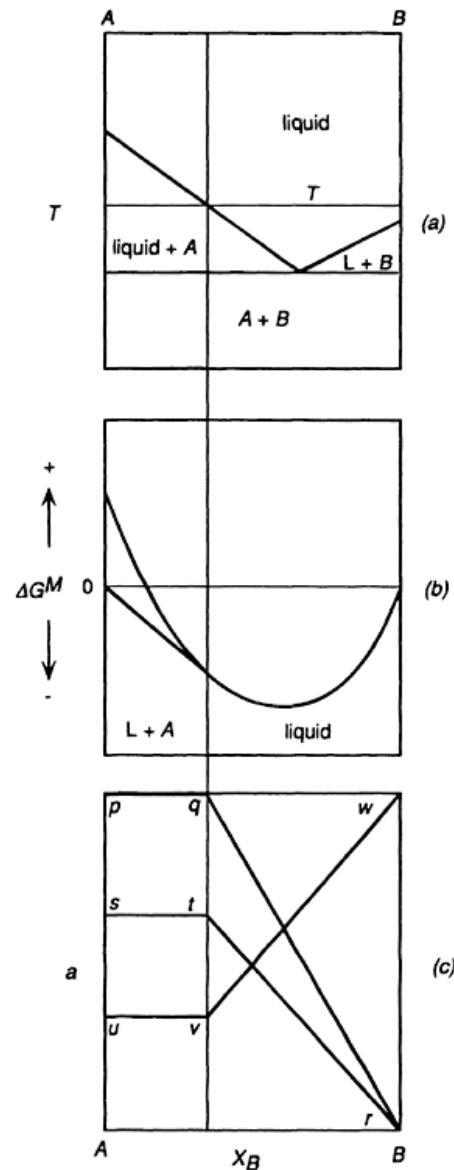
# 10. 6 Phase Diagrams, Gibbs Free Energy, and Thermodynamic Activity



**Figures 10.11–10.14** The effect of temperature on the molar Gibbs free energies of mixing and the activities of the components of the system  $A-B$ .



# 10. 6 Phase Diagrams, Gibbs Free Energy, and Thermodynamic Activity



The Gibbs free energy of formation of the liquid solutions in the system  $A-B$  at the temperature  $T$  is shown in Fig. 10.15*b*. The “double tangent” to the a solid solution and liquid solution curves is reduced to a tangent drawn from the point on the  $X_A=1$  axis which represents pure solid  $A$  to the liquid solutions curve. The corresponding activity-composition relations are shown in Fig. 10.15*c*. Again these are drawn in accordance with the supposition the the liquid solutions are ideal. In Fig. 10.15(*c*)  $pqr$  is the activity of  $A$  with respect to pure solid  $A$  at  $p$ ,  $s$  is the activity of pure liquid  $A$  with respect to solid  $A$  at  $p$ ,  $str$  is the activity of  $A$  with respect to liquid  $A$  having unit activity at  $s$ , and  $Auvw$  is the activity of  $B$  with respect to liquid  $B$  having unit activity at  $w$ .

In a binary system which exhibits complete miscibility in the liquid state and virtually complete immiscibility in the solid state, e.g., Fig. 10.15*a*, the variations of the activities of the components of the liquid solutions can be obtained from consideration of the liquidus curves. At any temperature  $T$  (Fig. 10.15*a*), the system with a composition between pure  $A$  and the liquidus composition exists as virtually pure solid  $A$  in equilibrium with a liquid solution of the liquidus composition.

**Figure 10.15** The molar Gibbs free energy of mixing and the activities in a binary eutectic system that exhibits complete liquid miscibility and virtually complete solid immiscibility.

## 10. 6 Phase Diagrams, Gibbs Free Energy, and Thermodynamic Activity

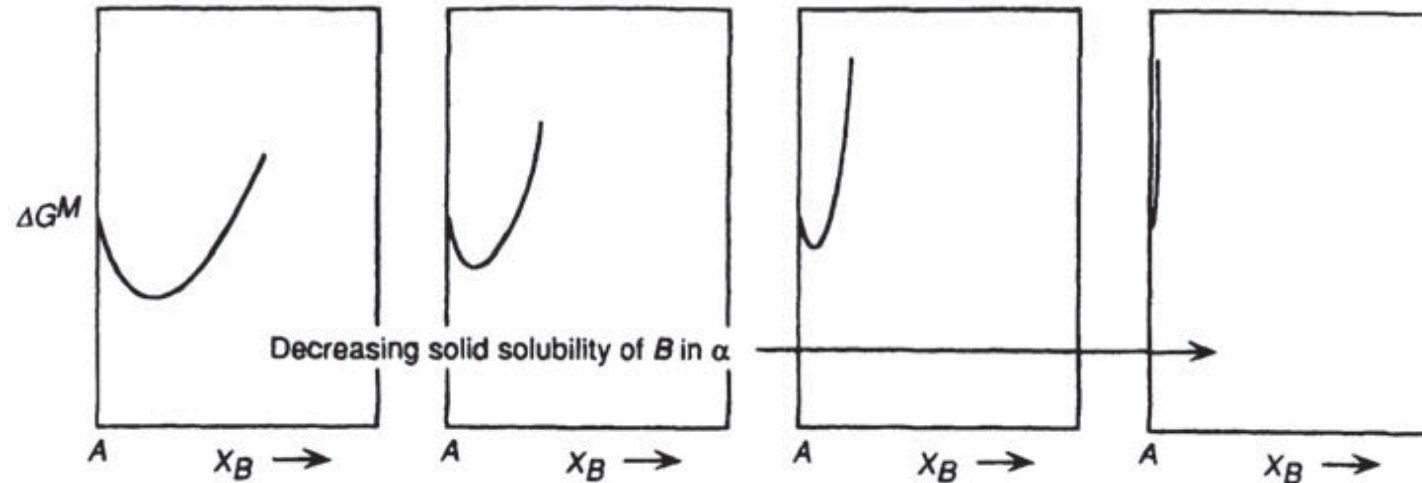


**Figure 10.16** The effect of decreasing solid solubility on the molar Gibbs free energy of mixing curve.

At any temperature  $T$  (Fig. 10.15*a*), the system with a composition between pure  $A$  and the liquidus composition exists as virtually pure solid  $A$  in equilibrium with a liquid solution of the liquidus composition. Thus, at  $T$

$$\begin{aligned} G_{A(s)}^{\circ} &= \bar{G}_{(l)}^A \\ &= G_{A(l)}^{\circ} + RT \ln a_A \end{aligned}$$

in which  $a_A$  is with respect to liquid  $A$  as the standard state. Thus

$$\Delta G_{m(A)}^{\circ} = -RT \ln a_A \quad (10.23)$$

or, if the liquid solutions are Raoultian,

$$\Delta G_{m(A)}^{\circ} = -RT \ln X_A \quad (10.24)$$

# 10. 6 Phase Diagrams, Gibbs Free Energy, and Thermodynamic Activity

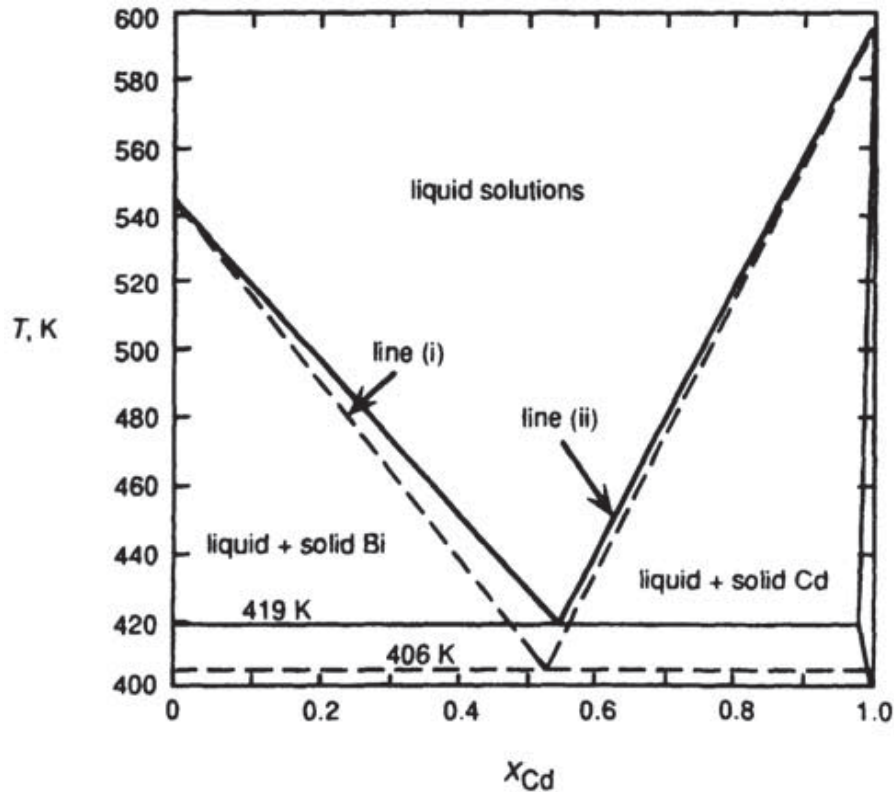


**Figure 10.17** The phase diagram for the system Bi–Cd. The full lines are the measured liquidus lines, and the broken lines are calculated assuming no solid solution and ideal mixing in the liquid solutions.

$$\Delta H_{m(\text{Bi})}^{\circ} = 10,900 \text{ J at } T_{m(\text{Bi})} = 554 \text{ K, and thus}$$

$$\Delta S_{m(\text{Bi})}^{\circ} = \frac{10,900}{544} = 20.0 \text{ J/K at } 544 \text{ K}$$

The molar constant pressure heat capacities of solid and liquid bismuth vary with temperature as

$$c_{p,\text{Bi}(s)} = 18.8 + 22.6 \times 10^{-3} T \text{ J/K}$$

$$c_{p,\text{Bi}(l)} = 20 + 6.15 \times 10^{-3} T + 21.1 \times 10^5 T^{-2} \text{ J/K}$$

Thus

$$c_{p,\text{Bi}(l)} - c_{p,\text{Bi}(s)} = \Delta c_{p,\text{Bi}} = 1.2 - 16.45 \times 10^{-3} T + 21.1 \times 10^5 T^{-2} \text{ J/K}$$

and

$$\begin{aligned} \Delta G_{m(\text{Bi})}^{\circ} &= \Delta H_{m(\text{Bi}),544}^{\circ} + \int_{554}^T \Delta c_{p,\text{Bi}} dT - T \left( \Delta S_{m(\text{Bi}),544}^{\circ} + \int_{544}^T \frac{\Delta c_{p,\text{Bi}}}{T} dT \right) \\ &= 16,560 - 23.79 T - 1.2 T \ln T + 8.225 \times 10^{-3} T^2 - 10.55 \times 10^5 T^{-1} \\ &= -RT \ln X_{\text{Bi}(\text{liquidus})} \end{aligned} \quad (10.25)$$

or

$$\ln X_{\text{Bi}(\text{liquidus})} = \frac{-1992}{T} + 2.861 + 0.144 \ln T - 9.892 \times 10^{-4} T + 1.269 \times \frac{10^5}{T^2}$$

# 10. 6 Phase Diagrams, Gibbs Free Energy, and Thermodynamic Activity

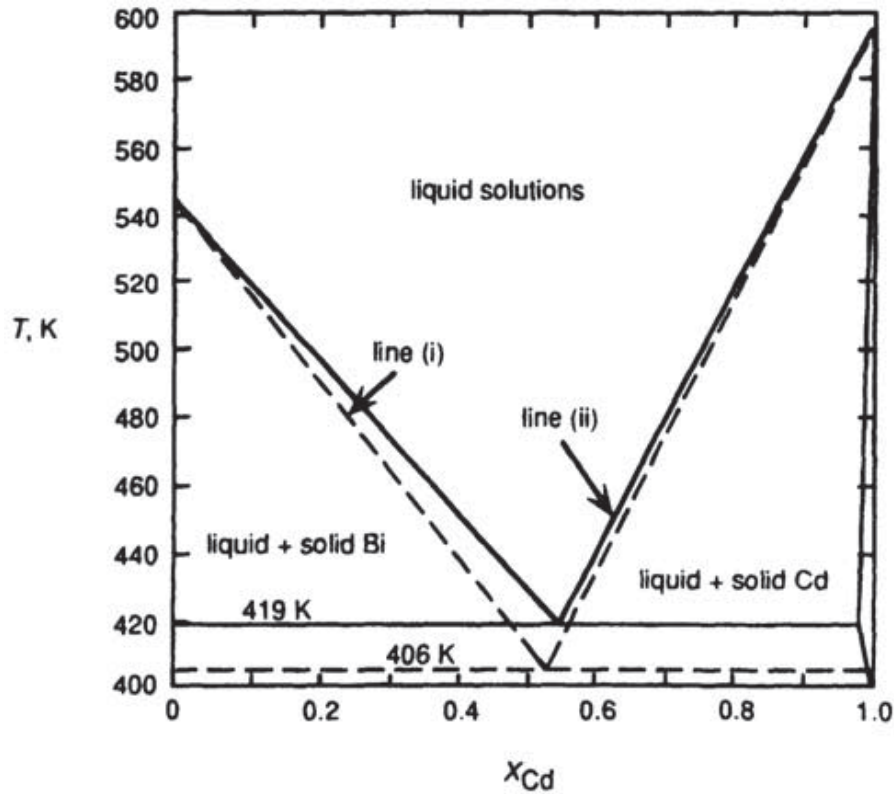


**Figure 10.17** The phase diagram for the system Bi–Cd. The full lines are the measured liquidus lines, and the broken lines are calculated assuming no solid solution and ideal mixing in the liquid solutions.

if the small solid solubility of Bi in Cd is ignored,

$$\Delta G_{m(\text{Cd})}^{\circ} = -RT \ln X_{\text{Cd}(\text{liquidus})}$$

$\Delta H_{m(\text{Cd})}^{\circ} = 6400\text{J}$  at  $T_{m,\text{Cd}} = 594\text{K}$  and thus  $\Delta S_{m(\text{Cd})}^{\circ} = \frac{6400}{594} = 10.77\text{J/K}$  at 594K. The constant pressure molar heat capacities are

$$c_{p,\text{Cd}(\text{s})} = 22.2 + 12.3 \times 10^{-3}T \text{ J/K}$$

and

$$c_{p,\text{Cd}(\text{l})} = 29.7 \text{ J/K}$$

Thus

$$c_{p,\text{Cd}(\text{l})} - c_{p,\text{Cd}(\text{s})} = \Delta c_{p,\text{Cd}} = 7.5 - 12.3 \times 10^{-3}T \text{ J/K}$$

$$\begin{aligned} \Delta G_{m(\text{Cd})}^{\circ} &= \Delta H_{m(\text{Cd}),594}^{\circ} + \int_{594}^T \Delta c_{p,\text{Cd}} dT - T \left( \Delta S_{m(\text{Cd}),594}^{\circ} + \int_{594}^T \frac{\Delta c_{p,\text{Cd}}}{T} dT \right) \\ &= 4155 + 37.32T - 7.5T \ln T + 6.15 \times 10^{-3}T^2 \text{ J} \quad (10.26) \\ &= -RT \ln X_{\text{Cd}(\text{liquidus})} \end{aligned}$$

or

$$\ln X_{\text{Cd}(\text{liquidus})} = \frac{-495}{T} - 4.489 + 0.90 \ln T - 7.397 \times 10^{-4}T$$

## 10. 6 Phase Diagrams, Gibbs Free Energy, and Thermodynamic Activity

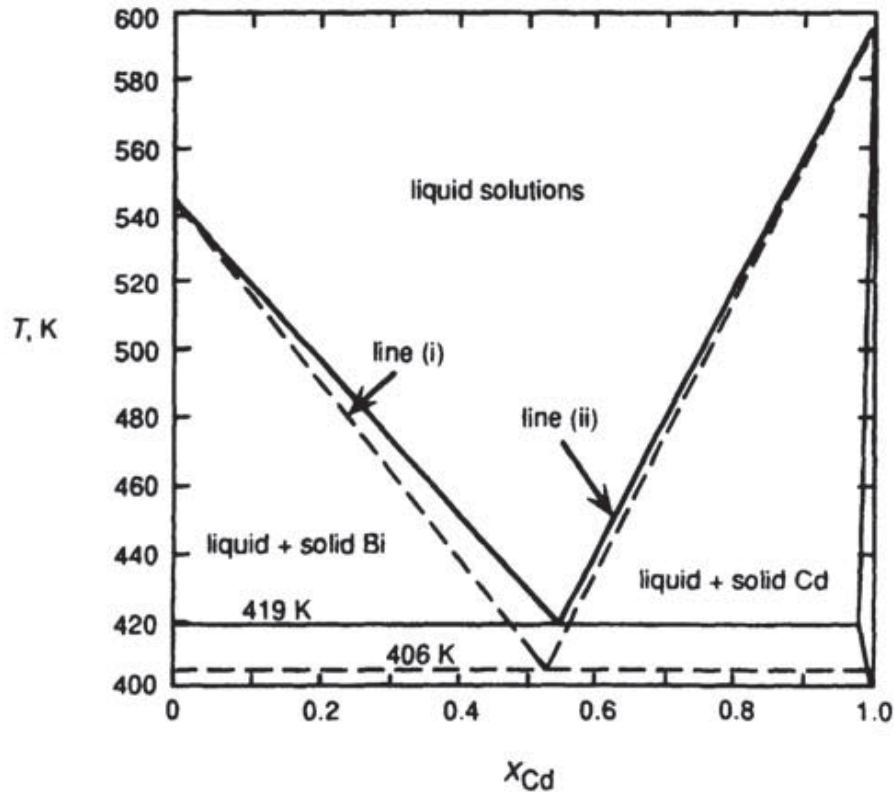


**Figure 10.17** The phase diagram for the system Bi–Cd. The full lines are the measured liquidus lines, and the broken lines are calculated assuming no solid solution and ideal mixing in the liquid solutions.

From Eq. (10.25),  $\Delta G_{m(\text{Bi}),419\text{K}}^0 = 2482\text{J}$ , and from Eq. (10.26),  $\Delta G_{m(\text{Cd}),419\text{K}}^0 = 1898\text{J}$ . Thus, from Eq. (10.23), in the actual eutectic melt,

$$a_{\text{Bi}} = \exp\left(\frac{-2482}{8.3144 \times 419}\right) = 0.49$$

and

$$a_{\text{Cd}} = \exp\left(\frac{-1898}{8.3144 \times 419}\right) = 0.58$$

The actual eutectic composition is  $X_{\text{Cd}}=0.55$ ,  $X_{\text{Bi}}=0.45$ , and thus the activity co-efficients are

$$\gamma_{\text{Bi}} = \frac{0.49}{0.45} = 1.09$$

and

$$\gamma_{\text{Cd}} = \frac{0.58}{0.55} = 1.05$$

Thus, positive deviations from Raoultian ideality cause an increase in the liquidus temperatures.

# 10. 6 Phase Diagrams, Gibbs Free Energy, and Thermodynamic Activity

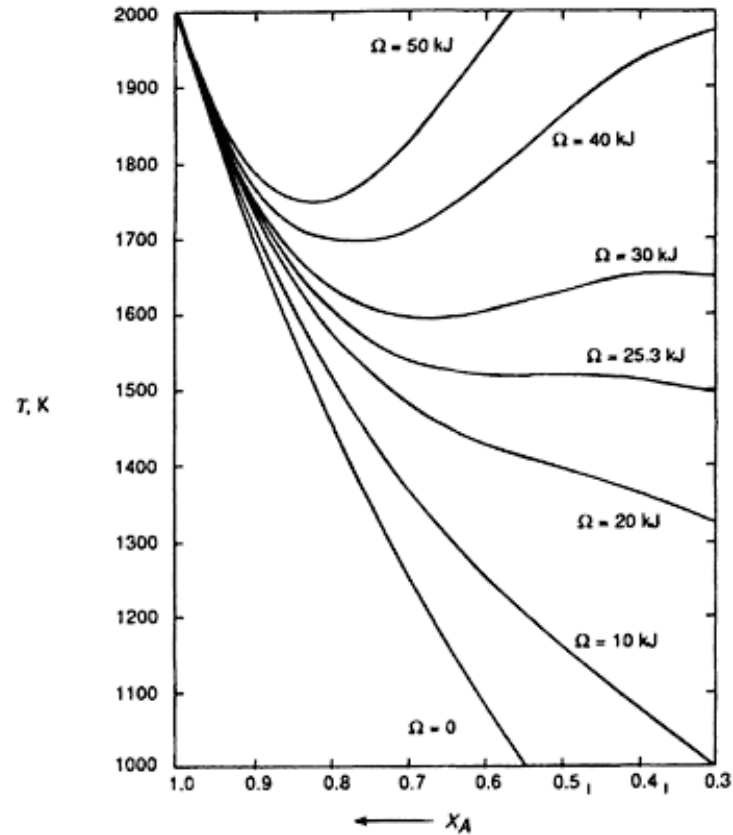


**Figure 10.18** Calculated liquidus lines assuming regular solution behavior in the liquid solutions and no solid solubility.

Assuming regular solution behavior, Eq. (10.23), written in the form

$$-\Delta G_{m(A)}^{\circ} = RT \ln X_A + RT \ln \gamma_A$$

$$-\Delta G_{m(A)}^{\circ} = RT \ln X_A + RT\alpha(1 - X_A)^2$$

from Eq. (9.90),

$$-\Delta G_{m(A)}^{\circ} = RT \ln X_A + \Omega(1 - X_A)^2 \quad (10.27)$$

Consider a hypothetical system  $A-B$  in which  $\Delta H^0 = 10\text{kJ}$  at  $T_{m,A} = 2000\text{K}$ . Thus, for this system

$$-10,000 + 5T = RT \ln X_A + \Omega(1 - X_A)^2$$

where  $X_A$  is the composition of the  $A$  liquidus at the temperature  $T$ . The  $A$  liquidus lines, drawn for  $\Omega=0, 10, 20, 25.3, 30, 40,$  and  $50$  kJ, are shown in Fig. 10.18. As  $\Omega$  exceeds some critical value (which is  $25.3$  kJ in this case), the form of the liquidus line changes from a monotonic decrease in liquidus temperature with decreasing  $X_A$  to a form which contains a maximum and a minimum. At the critical value of  $\Omega$  the maximum and minimum coincide at  $X_A=0.5$  to produce a horizontal inflexion in the liquidus curve. It is apparent that, when  $\Omega$  exceeds the critical value, isothermal tie-lines cannot be drawn between pure solid  $A$  and all points on the liquidus lines, which, necessarily, means that the calculated liquidus lines are impossible.

# 10. 6 Phase Diagrams, Gibbs Free Energy, and Thermodynamic Activity

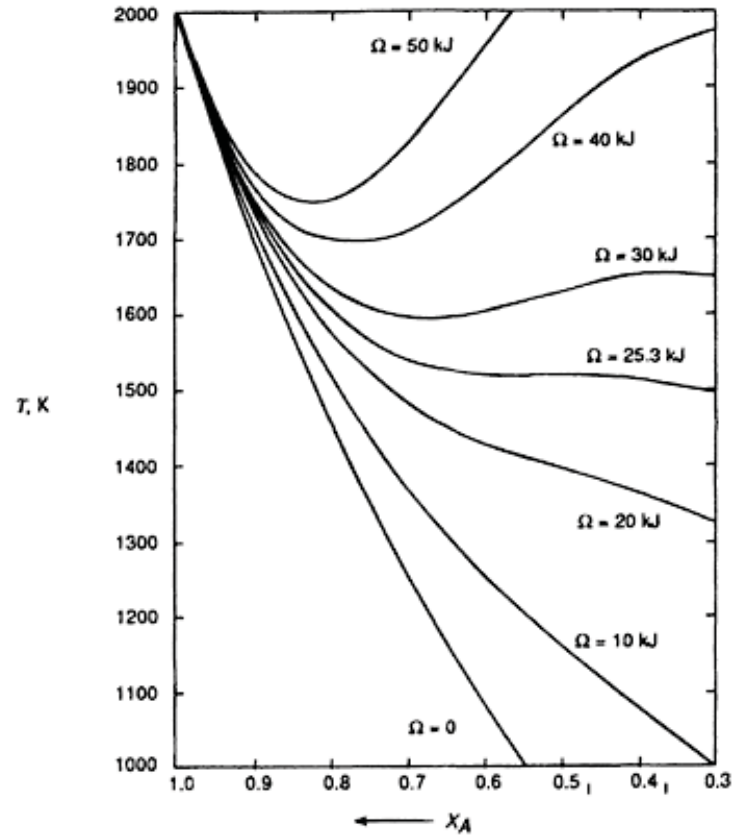


**Figure 10.18** Calculated liquidus lines assuming regular solution behavior in the liquid solutions and no solid solubility.

From Eq. (10.21)

$$\ln a_A = \frac{-\Delta H_{m(A)}^\circ}{RT} + \frac{\Delta H_{m(A)}^\circ}{RT_{m(A)}}$$

Thus

$$d \ln a_A = \frac{da_A}{a_A} = \frac{\Delta H_{m(A)}^\circ}{RT^2} dT$$

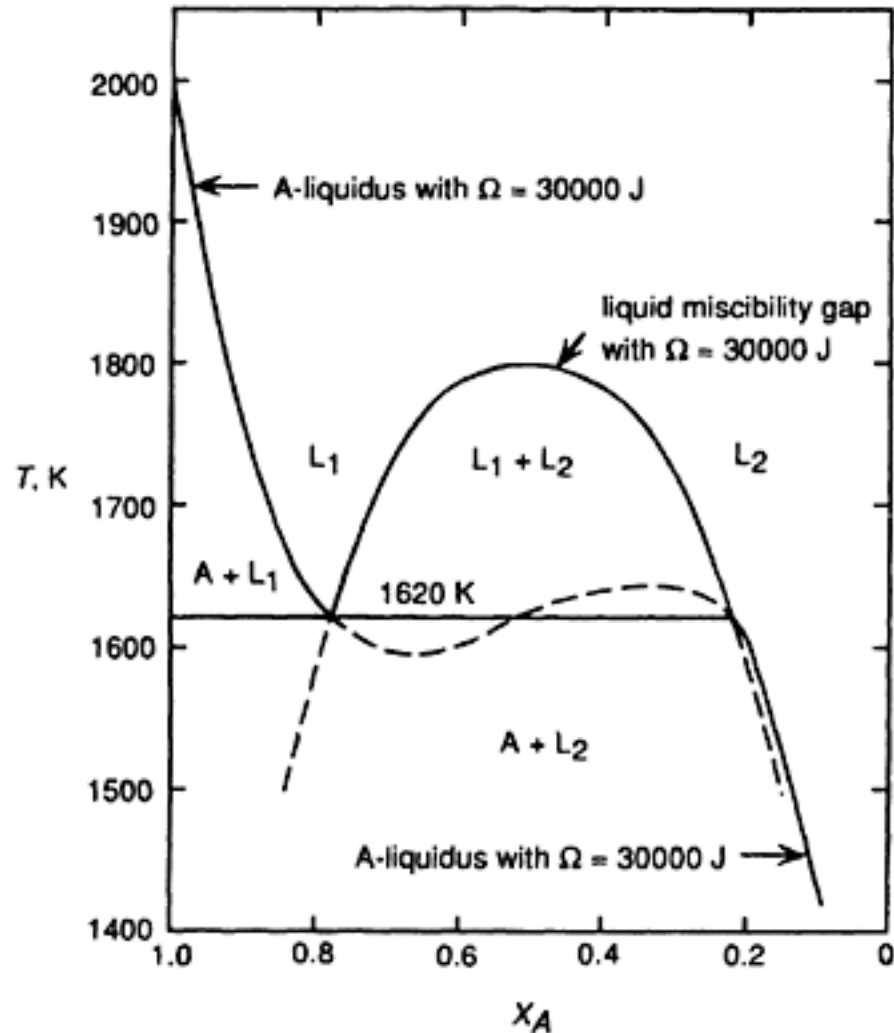
or

$$\frac{dT}{dX_A} = \frac{RT^2}{\Delta H_{m(A)}^\circ a_A} \frac{da_A}{dX_A} \quad (10.28)$$

and also

$$\frac{d^2T}{dX_A^2} = \frac{2RT}{\Delta H_{m(A)}^\circ a_A} \frac{da_A}{dX_A} \frac{dT}{dX_A} - \frac{RT^2}{\Delta H_{m(A)}^\circ a_A^2} \left( \frac{da_A}{dX_A} \right)^2 + \frac{RT^2}{\Delta H_{m(A)}^\circ a_A} \frac{d^2a_A}{dX_A^2} \quad (10.29)$$

## 10. 6 Phase Diagrams, Gibbs Free Energy, and Thermodynamic Activity



$$\alpha_{cr} = \frac{\Omega_{cr}}{RT_{cr}} = \frac{25,390}{8.3144 \times 1413} = 2$$

The phase equilibria generated when  $\Omega > \Omega_{cr}$  are shown in Fig. 10.19 which shows the immiscibility in regular liquid solutions with  $\Omega = 30,000$  J and the A-liquidus for  $\Omega = 30,000$  J shown in Fig. 10.18.

The liquid immiscibility curve and the A-liquidus curve intersect at 1620 K to produce a three-phase monotectic equilibrium between A and liquidus  $L_1$  and  $L_2$ . The liquid immiscibility curve is metastable at temperatures less than 1620 K, and the calculated A-liquidus is physically impossible between the compositions of  $L_1$  and  $L_2$  at 1620 K.

Figure 10.19 The monotectic equilibrium in a binary system in which the liquid solutions exhibit regular solution behavior with  $\Omega = 30,000$  J.



# 10.7 The Phase Diagrams of Binary Systems That Exhibit Regular Solution Behavior in The Liquid and Solid States

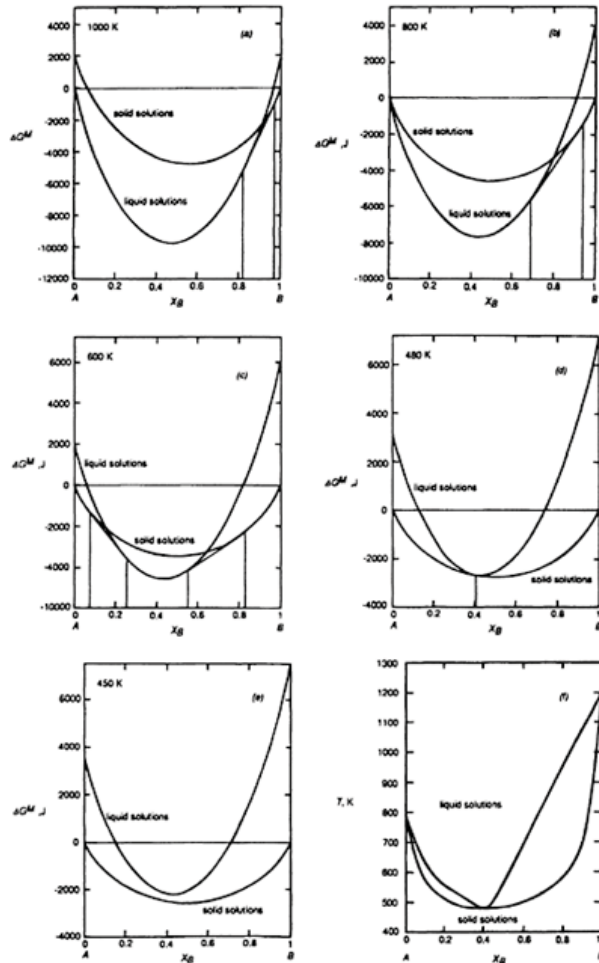


**Figure 10.20** The Gibbs free energy of mixing curves at various temperatures, and the phase diagram for a binary system which forms regular solid solutions in which  $\Omega_s=0$  and regular liquid solutions in which  $\Omega_l=-20,000$  J.

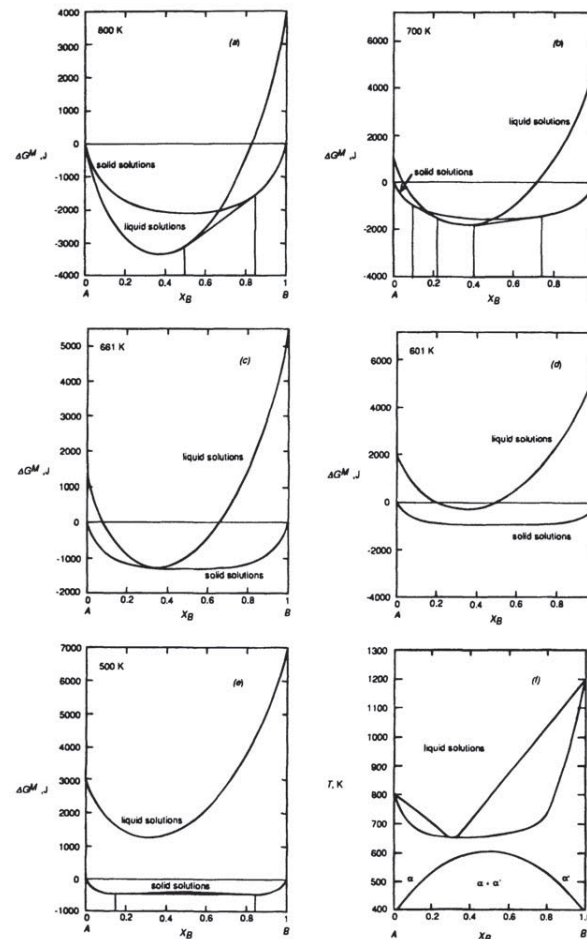


**Figure 10.21** The Gibbs free energy of mixing curves at various temperatures, and the phase diagram for a binary system which forms regular solid solutions in which  $\Omega_s=10,000$  J and regular liquid solutions in which  $\Omega_l=-2000$  J.

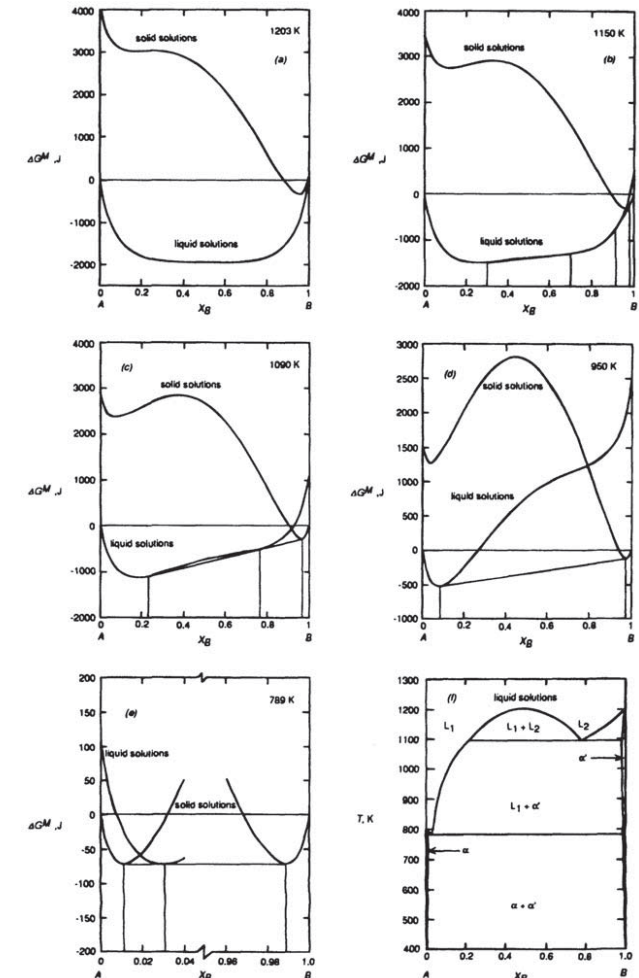


**Figure 10.22** The Gibbs free energy of mixing curves at various temperatures, and the phase diagram for a binary system which forms regular solid solutions in which  $\Omega_s=30,000$  J and regular liquid solutions in which  $\Omega_l=20,000$  J.

# 10.7 The Phase Diagrams of Binary Systems That Exhibit Regular Solution Behavior in The Liquid and Solid States

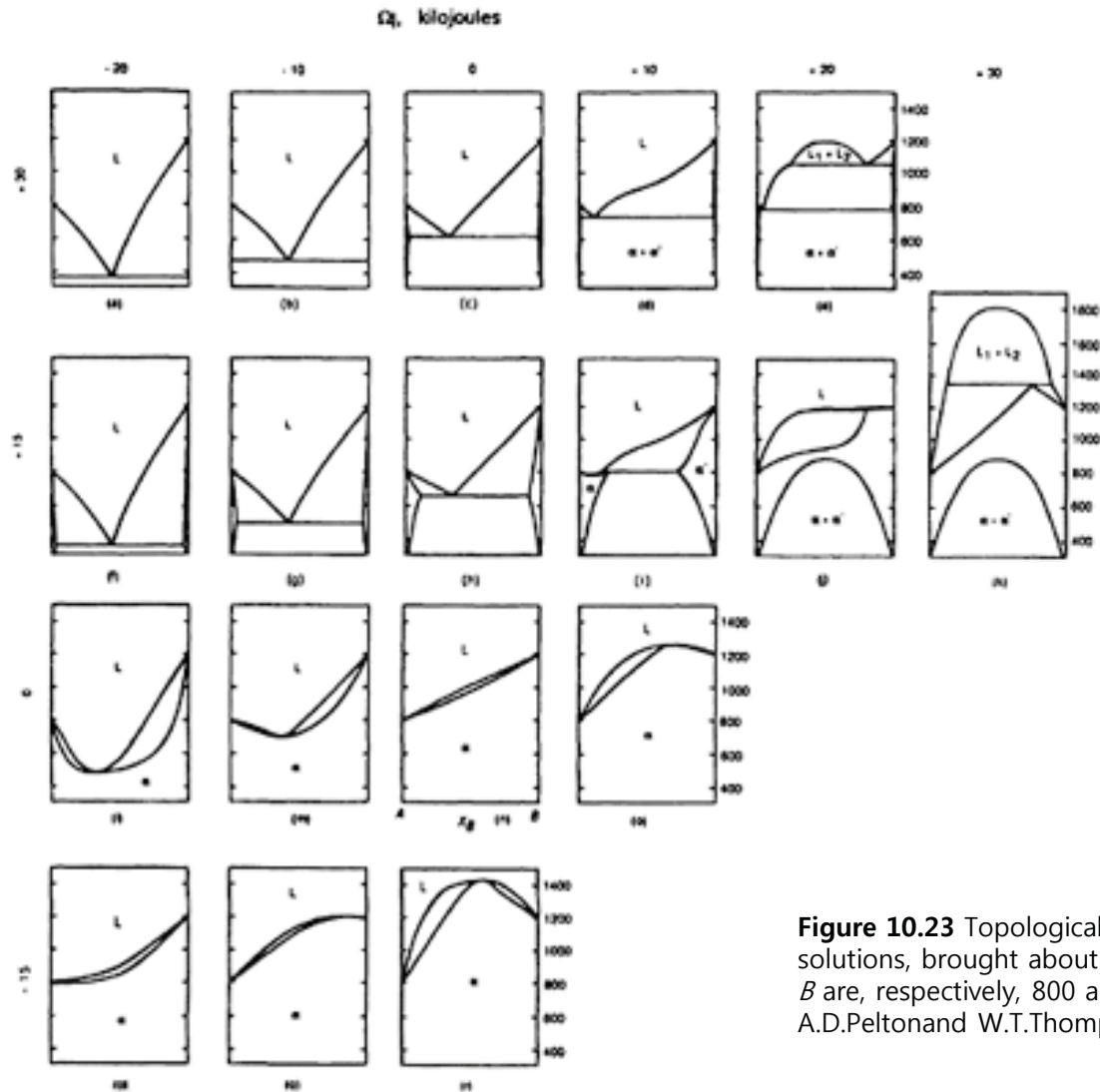


**Figure 10.23** Topological changes in the phase diagram for a system  $A-B$  with regular solid and liquid solutions, brought about by systematic changes in the values of  $\Omega_s$  and  $\Omega_l$ . The melting temperatures of  $A$  and  $B$  are, respectively, 800 and 1200 K, and the molar entropies of melting of both components are 10 J/K. (From A.D.Pelton and W.T.Thompson, *Prog. Solid State Chem.* (1975), vol. 10, part 3, p. 119).